Proceedings of the 10th Brazilian Congress of Thermal Sciences and Engineering -- ENCIT 2004
Braz. Soc. of Mechanical Sciences and Engineering -- ABCM, Rio de Janeiro, Brazil, Nov. 29 -- Dec. 03, 2004

Paper CIT04-0811

MODELLING THE HYDROTHERMODYNAMICS OF THE SURFACE LAYER OF A STRATIFIED TROPICAL SUBTROPICAL OCEAN

Carlos A. A. Carbonel H.
Laboratório Nacional de Computação Científica (LNCC) .
Av. Getulio Vargas 333, Cep: 25651-070 Petrópolis, RJ ,Brazil.
e-mail : carbonel@lncc.br,

Augusto C. N. Galeão
Laboratório Nacional de Computação Científica (LNCC) .
Av. Getulio Vargas 333, Cep: 25651-070 Petrópolis, RJ ,Brazil.
e-mail : acng@lncc.br

***Abstract**. In the present paper, a two-layer model is developed for the non-permanent hydrothermodynamics of a tropical subtropical coastal ocean. The model includes the conservation equations of motion, continuity and heat. The equations apply only to the thin and warm oceanic surface layer. The deep layer is stipulated to be motionless and arbitrarily deep and separated from the upper layer by a density discontinuity. Cold deep water is carried across the interface from the lower into the upper layer; it becomes warmed up there by the net energy input from the atmosphere into the ocean The non-uniform sea surface wind stress and heat at the surface are the main forcing functions of the model.*
A numerical finite element method is proposed to approach the hydrothermodynamic problem. The model uses simple linear spatial and temporal continuous polynomials. A stabilising Petrov-Galerkin operator to improve the classical finite element Galerkin approach is considered.
The hydrothermodynamic response is obtained for the eastern pacific boundary in the southern hemisphere. Monthly climatological data are used to determine the wind and heat fluxes forcings of the model for the month of February. The model is successful in simulating the main features of the observed SST pattern. In particular, the model develops upwelling along the coastal boundary, the warm water intrusion in offshore side and signals of countercurrents.

***Keywords**. Hydrothermodynamics, Ocean models, Eastern ocean boundaries, Finite elements, Petrov-Galerkin formulation.*

1. Introduction

The most familiar characteristic of eastern boundary currents (EBCs), is the importance of equatorward surface currents and coastal upwelling resulting from a predominantly equatorward wind stress. The EBCs feature large stocks of small pelagic fishes, which provide about one third of the world's total catch of fish. Also the EBCs have some commonality in their physical structure and the mechanisms that force their oceanographic character (Parrish et al., 1983; Lluch-Belda et al., 1992). The existence of undercurrents is a dynamical feature that increase the complexity of the eastern boundary ocean dynamics.

In order to interpret this dynamics, and provide a dynamical basis for its prediction, it is necessary to consider the circulation in a large extended area of the eastern oceans. A important issue is to develop a hydrodynamic model which shows that upwelling, the horizontal circulation and sea surface temperature (SST) fields are associated phenomena. A first contribution to the circulation in the eastern tropical oceans was provided by Yoshida (1967), discussing a theoretical permanent two layer model, that qualitatively reproduces the topography of sea surface, thermocline, and poleward coastal underrcurrents which are dynamically related to upwelling.

Past numerical studies in the 70's were developed for the eastern pacific ocean (e.g. Hulburt, 1974; O'Brien et. Al. 1979; Preller and O'Brien, 1980) using the finite difference method (FDM). In these studies, oriented to the upwelling response, the influence of the coastline geometry and bottom topography were focussed. Despite remarkable achievements gained with the finite element method (FEM) in simulating coastal and tidal dynamics, ocean general circulation models (OGCMs) used in climatic studies still almost exclusively rely on the FDM. The only exception is the spectral element ocean model (SEOM) (Iskandarani et al., 1995). One of the main problems to use FEM models is that the change in grid spacing gives rise to unphysical wave scattering that is not dangerous for steady state engineering problems or for ocean circulation problems at relatively short integration time (as is the case for tide and coastal models) but might become of crucial importance for modelling large-scale ocean circulation. The resolution in coastal region of these models is also a problem due the extend of the models.

But the problem of unphysical wave scattering could be solved using variational formulations that include streamline upwind Petrov-Galerkin (SUPG) and similar operators. Finite element formulations using SUPG and similar operators to improve the Galerkin classical solution, were initially proposed for advection-difusion and compressible flow problems (e.g. Brooks and Hughes, 1982; Shakib, 1988; Almeida, Galeão, Silva, 1996). Formulations using a symmetric form of the shallow water wave equations were reported in last years (e.g. Bova and Carey,1995; Carbonel, Galeão and Loula, 2000). Also for hydrodynamic baroclinic circulation, an approach was recently presented (Carbonel and Galeão 2004) focussing the wind-driven dynamic response in open and limited areas.

Here, a finite element 1 ½ layer model of limited area domain, that includes the hydrodynamic and thermodynamic of the surface ocean layer is proposed to describe the upper layer dynamics in the eastern boundary pacific ocean. The variational formulation of Petrov-Galerkin is applied to improve the classical Galerkin approach.

The model is restricted to the region of interest , a difference with other models that need to describe all the pacific ocean. The model is forced by fields of wind and heat fluxes at the surface. Obviously the eastern pacific coastal current system have a complicated vertical structure and current configuration; therefore, the present study is a first step in the study of the eastern pacific ocean. Our main purpose here is to prove the ability of the proposed model evaluating the surface tendency response under action of mean forcing functions. Also, it is very important to determine in what a magnitude the observed features of the SST depends on the mentioned forcings only.

The pacific coast is a typical upwelling region due the permanent favourable winds. During the summer months the coastal upwelling continues, but warming waters from the north invaders the region in the offshore side mainly. The Figure 1 (left panel) shows the mean SST for February in the eastern pacific ocean (Da Silva et.al, 1994). It is noted that warmer water occupied an important part of the region. The contour of 23^{o}C describes a warm plume that reaches the 20^{o}S. Colder water are observed in the south side of the study area and along the coast between the 10^{o}S to 17^{o}S. The simultaneously existence of colder waters near the coast and a southward warmer intrusion offshore, configures strong SST gradients which are a challenger modelling coastal ocean processes. Therefore, here we focussed the modelling objectives to the evaluation of the hydro-thermodynamics for the summer month of February.

It is known that the dynamics of both wind stress and SST tend to be divided into three regions (Figure 1, right panel), with a transition zone that varies in extent through time, and whose dynamic alternately varies as one or the other adjacent zones. The north and south sectors have negative anomalies of SST whereas central sector has positive anomalies. A common trend that occurs also in the California current system (Mendelshon and Schwing, 2002).

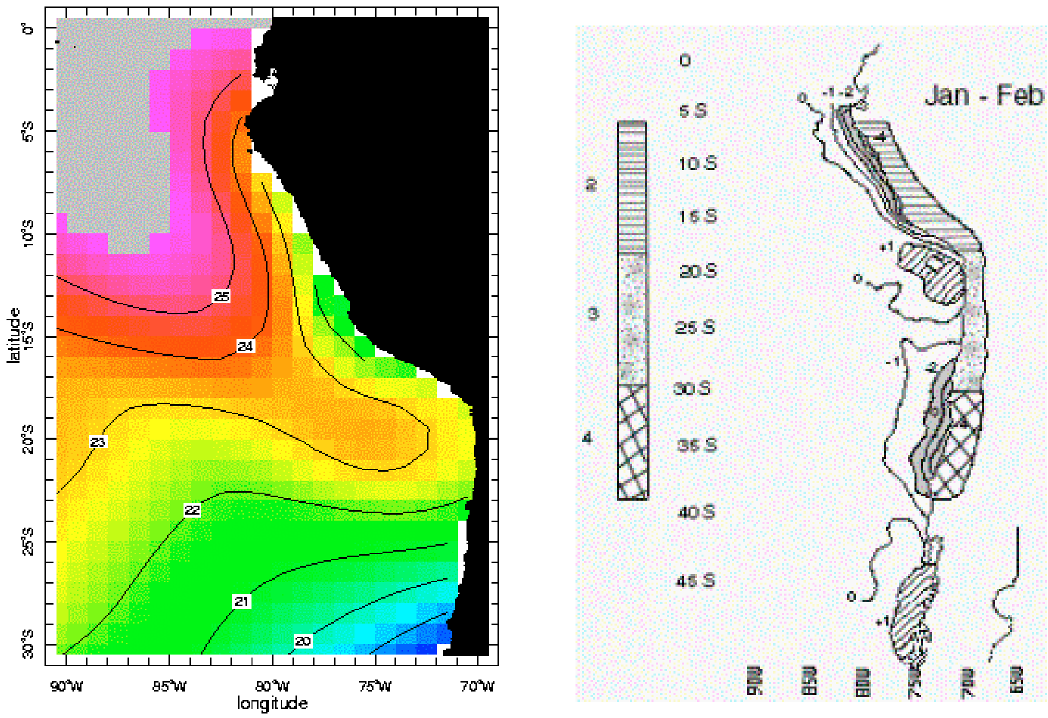

Figure 1. Left panel: The mean SST(^{o}C) for February in the eastern pacific ocean (from Da Silva et.al, 1994). Right panel: The SST anomalies corresponding to January February and the sectors 2, 3 and 4 along the Peru Chile coast (from Mendelshon and Schwing, 2002.

2. The ocean model

2.1 The governing equations

We use cartesian co-ordinates *x,y* oriented positively to the East and North respectively. A coastal ocean is defined in a domain Ω with land type boundary Γ_L and an ocean type boundary Γ_O. Two layers are consider to describe the vertical structure (Figure 2). The upper layer of density ρ^u with thickness *h* and an inert lower layer ρ^l , where it is assumed that the pressure gradient is zero. In that way the faster barotropic mode is eliminated and the first internal baroclinic mode is only consider. The thermal structure is defined by the instant upper layer temperature *T*, and the lower layer temperature T^l.

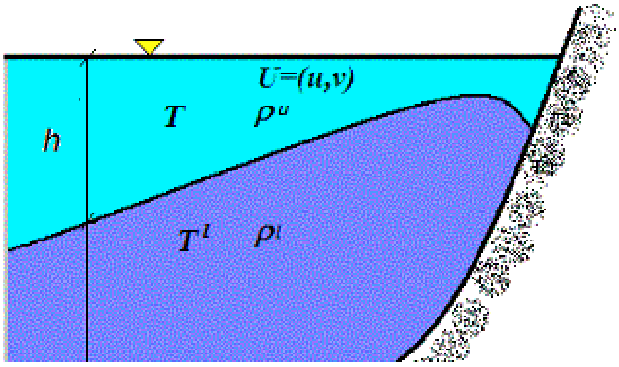

Figure 2. The two layers of the ocean system

As constitutive state equation is valid the *ansatz*

$$\rho^u = \rho^l[1-\alpha(T-T^l)] \tag{1}$$

where, *T* is the actual temperature and α the thermal expansion coefficient. Here, the influence of the salinity is not included without a loss of generality, because with temperature and salinity an apparent temperature could be estimated modifying only the constant α (Hantel, 1971; Fofonoff, 1962).

We define for convenience, the variables

$$d = 2c = 2\sqrt{g\sigma h} \;\;,\;\; b = \frac{c^0 T}{T^u} \tag{2}$$

which have velocity units, and are function of the upper layer thickness *h* and the upper layer temperature *T* respectively. The parameter *g* represent the acceleration gravity, $\sigma = 1 - \rho^u/\rho^l$, and $c^0 = \sqrt{g\sigma H}$ is a referential celerity function of the initial upper layer thickness *H*. T^u is the referential initial temperature in the upper layer.

The set of equations for the vector *V=(u,v,d,b)* are the following:

$$\frac{\partial V}{\partial t} + \underline{A}\frac{\partial V}{\partial x} + \underline{B}\frac{\partial V}{\partial y} + \underline{C}V + \underline{D}\left(\frac{\partial^2 V}{\partial x^2} + \frac{\partial^2 V}{\partial y^2}\right) + F = 0 \tag{3}$$

$$\underline{A}=\begin{pmatrix} u & 0 & c & s \\ 0 & u & 0 & 0 \\ c & 0 & u & 0 \\ 0 & 0 & 0 & u \end{pmatrix}, \underline{B}=\begin{pmatrix} v & 0 & 0 & 0 \\ 0 & v & c & s \\ 0 & c & v & 0 \\ 0 & 0 & 0 & v \end{pmatrix}, \underline{C}=\begin{pmatrix} 0 & -f & 0 & 0 \\ f & 0 & 0 & 0 \\ 0 & 0 & 0 & 0 \\ 0 & 0 & 0 & 0 \end{pmatrix},$$

$$\underline{D}=\begin{pmatrix} -\vartheta & 0 & 0 & 0 \\ 0 & -\vartheta & 0 & 0 \\ 0 & 0 & 0 & 0 \\ 0 & 0 & 0 & -\vartheta_T \end{pmatrix},\ F=\begin{pmatrix} -\tau_x / \rho^u h \\ -\tau_y / \rho^u h \\ -w_e g\sigma / c \\ (Q_I - Q)/h \end{pmatrix},\ V=\begin{pmatrix} u \\ v \\ d \\ b \end{pmatrix}$$

Where u, v are the velocity components in the upper layer. The entrainment velocity w_e, is approached by $w_e = (H_e - h)^2 / t_e H_e$, where H_e and t_e are the depth and time scales of the entrainment process. h is the upper layer thickness. The wind stress components are represented by τ_i , f is the Coriolis parameter that depends of the geographical co-ordinates. The parameters ρ^u , ρ^l , ρ_{air} are the densities in the upper layer, lower layer and air respectively. The parameters $\mu=\rho^u/\rho^l$, $\sigma = 1 - \mu$, and $\overline{\mu} = \mu/(\mu-\sigma)$ are density ratios. The sea surface temperature (SST) is T, the initial upper layer temperature is T^u, and T^l is the lower layer temperature. The parameter α is the coefficient of thermal expansion. The parameter $s = gh\theta T^u / 2\overline{\mu} c^0$, $c^0 = \sqrt{g\sigma H}$ is the referential wave celerity function of the initial layer thickness H. Q is the surface heat flux, and $Q_I = k_I (T - T^l)/h$, is the gain or loss of heat across the interface, depending of the dynamical convergence or divergence of the flows ω in the upper layer and the parameter $k_I = \omega H$ (Carbonel, 2003).

The thermodynamic part of the model is driven by the surface heat flux Q with is defined as

$$Q = Q_s - Q_{lw} - Q_e - Q_h \tag{4}$$

where Q_s is the net short wave radiation, Q_{lw} the resultant outgoing longwave radiation, $Q_h = \rho_{air} c_{pa} C_H (T - T_{air})|W|$ the sensible heat, and $Q_e = \rho_{air} C_e L (q - q_{air})|W|$ is the latent heat. Where L is the latent heat of evaporation, the parameter c_{pa} is the specific heat of the air, C_H, C_e are the Stanton parameter, and q is the saturation specific humidity,

To solve the equation system (3), on land type boundaries, we have non-slip boundary conditions for the velocities

$$u = v = 0 \tag{5}$$

and homogeneous conditions are assumed for upper thickness h and temperature T.

On an ocean boundary we prescribe a weakly reflective boundary condition, based on the characteristic method, in an axis normal (x_n) to the open boundary is defined as

$$\frac{DR^{\pm}}{Dt} = 0 \tag{6}$$

where the *Riemann* quasi-invariant $R^{\pm} = u_n \pm d$ are valid, along the characteristics $dx_n /dt = u_n \pm c$ normal to the open boundary. u_n represent the velocity component normal to the boundary. The weakly reflective conditions on the open boundary are defined by the in-going characteristic of the presented equations. The advantages of this kind of open boundaries modelling coastal upwelling was recently reported by Carbonel (2003).

For the Temperature at the open boundaries, homogeneous condition is assumed.

For the initial conditions, an appropriate initial state is necessary to be assumed in the domain Ω and at the boundary Γ:

$$u = u^o,\ v=v^o,\ h= h^o,\ T= T^o \qquad at \qquad t = 0 \tag{7}$$

where u^o, v^o, h^o and T^o represent the initial velocity components, thickness and temperature respectively.

2.2 Space time Petrov-Galerkin method (*STPG*)

A space-time Petrov-Galerkin finite element model the for the above ocean problem is constructed. We define a space-time finite element partition $\pi^{h,\Delta t}$, in which the time interval is partitioned into subintervals

$$I_n = t_{n+1} - t_n = \Delta t \ , \quad t \in (0,T] \tag{8}$$

where t_n , t_{n+1} belong to an ordered partition of time levels $0 = t_0 < ....t_n < t_{n+1}....< t_F = T$.

The space domain Ω is partitioned in N sub-domains Ω_e with boundary Γ_e , such that The space-time integration domain is the slab $S_n = \Omega \times I_n$ with boundary $\Gamma_n = \Gamma_e \times I_n$. Then , the resulting slab is composed by N elements $S_n^e = \Omega_e \times I_n$.

Let P_n^h the finite element space of piecewise polynomial in space and time on the slab S_n. Defining

$$U_n^h = \{V^h \in P_n^h \times P_n^h; V^h = \overline{V}^h \; on \; \Gamma\} \tag{9a}$$

$$\hat{U}_n^h = \{\hat{V}^h \in P_n^h \times P_n^h; \hat{V}^h = 0 \; on \; \Gamma\} \tag{9b}$$

where V^h is the approximate solution and $\hat{V}^h$ the interpolation function. Here, continuous and linear interpolation in space and time will be considered.

The residual vector of the equation system (3) reads,

$$R^h = \underline{I}\frac{\partial V^h}{\partial t} + \underline{A}(V^h)\frac{\partial V^h}{\partial x} + \underline{B}(V^h)\frac{\partial V^h}{\partial y} + \underline{C}(V^h) + \underline{D}(\frac{\partial^2 V^h}{\partial x^2} + \frac{\partial^2 V^h}{\partial y^2}) + F \tag{10}$$

Then, we say that the space-time Petrov-Galerkin approximate solution for the hydro-thermodynamic problem is the vector $V^h \in U_n^h$, which satisfies $\forall \hat{V}^h \in \hat{U}_n^h$, the following equation

$$\int_{S_n} \hat{V}^h R^h \, d\Omega dt + \sum_{e=1}^{N} \int_{S_n^e} \overline{\Psi}_e \, G^h R^h \, d\Omega dt = 0 \tag{11}$$

where

$$G^h = \underline{I}\frac{\partial \hat{V}^h}{\partial t} + \underline{A}(V^h)\frac{\partial \hat{V}^h}{\partial x} + \underline{B}(V^h)\frac{\partial \hat{V}^h}{\partial y} \tag{12}$$

is a space-time operator and

$$\overline{\Psi}_e = \sum_{k=1}^{3} \gamma_k e_k e_k^T \tag{13}$$

is the stabilising matrix. The parameter

$$\gamma_k = 1/\sqrt{\lambda_k} \tag{14}$$

are the eigenvalues of the matrix

$$[(1/\Delta t)^2 \underline{I} + (1/l_x^2)\underline{A}^2 + (1/l_y^2)\underline{B}^2]^{-1/2} \tag{15}$$

and e_k their eigenvectors (see Shakib, 1988; Bova and Carey, 1995). The parameter l_x , l_y are the characteristics lengths of the finite element. The algebraic equation system is solved using the direct method of Gauss.

3. The SST response in the eastern boundary pacific ocean

The study area for the modelling purposes is showed in Figure 3 and extends from the equator to the 30°S. The extend in the west-east direction is from the 70° W to 90° W.

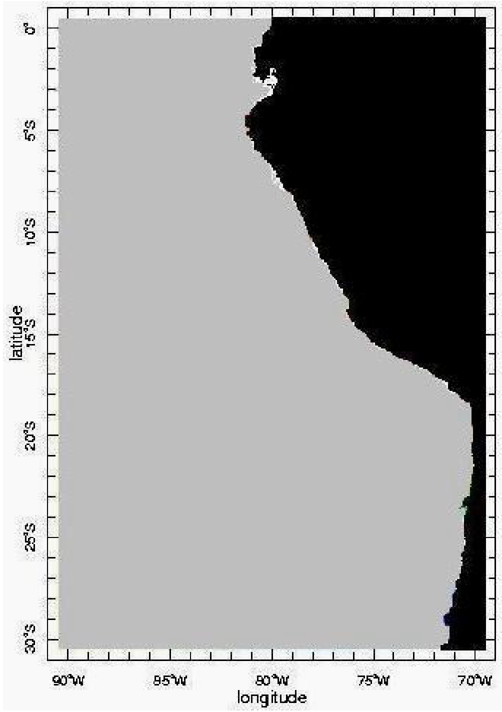

Figure 3. The eastern pacific ocean

There are diverse coastal irregularities, but for our schematised model, we only consider the irregularities located at 5°S and at 19°S. The other coastal irregularities, for example, the Guayaquil Bay (3°S), and the coastline change located at the Paracas peninsula (14°S) could be added in a next study focussing the detailed role of the indicated coastal configurations in the regional pattern.

The model coastline is a simple schematised configuration of the pacific coast from de 30°S to 0°S, described by straight lines connecting 4 points from south to north 70°W, 30°S; 70°W, 18.6°S; 81°W, 6°S; 81°W, 0°S. The domain is composed 1810 nodes and 3419 triangular linear elements (Figure 4).

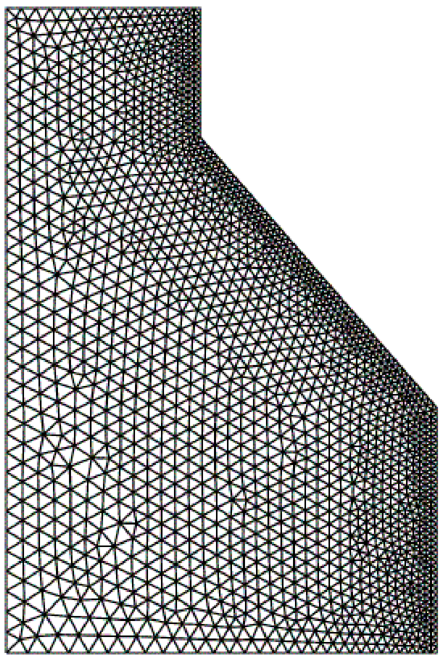

Figure 4. Finite element mesh of the schematised eastern pacific coastal ocean

The un-structured finite element mesh is fine near the coastline, whereas the mesh is coarser offshore. The smaller sides of the elements along the coastline are of 0.3^o , whereas in the left outer boundary the side elements are up to 0.9^o.

In this section, a numerical experiment is performed evaluating the dynamic of the coastal ocean. The basic parameter values used in the experiment are the following: The fluids in the layers are initially at rest. The time step is defined as Δt = 10800sec . The densities of the upper and lower layer are ρ^u=1024 kg m^{-3} and ρ^l=1025.5 kgm^{-3}, ρ_{air}=1.175 kg m^{-3} The free parameter in the stabilising term is calculated according to Eq. (13). The initial upper layer thickness is H=50 m. The entrainment depth H_e=30m and the entrainment time scale t_e =0.5 days, a value that is good for modelling in smaller space scale (Carbonel, 2003), but here is used too. The initial upper temperature T^u =26^o C, and the lower layer temperature is defined as T^u =14^o C.

In the experiment, the forcing functions of the model are the February monthly mean fields for the wind velocity, net incident heat flux (Q_n =Q_s - Q_{lw}), the air temperature T_{air}, and the specific humidity q_{air} . These forcings are extracted from the Atlas of Da Silva et. al. (1994). It is necessary to remark, that in the evaluation of the surface heat flux Q (Eq. 4), the contributions Q_e and Q_h, are obtained using the water temperature T from the model, instead the observed SST. The parameter used for evaluation of Q_e and Q_h are the following: The latent heat of evaporation is L = 2.44 x10^6 J/kg, the parameter C_H, C_e are equal to 0.0013, the specific heat of the air is c_{pa} = 1004 J/kg. The saturation specific humidity q is evaluated in function of the saturation vapour pressure e (see Rosenfeld et. al. 1994).

The fields Q_s ,Q_{lw} T_{air}, q_{air} for the schematised model were obtained by interpolation of the original data for each node of the schematised ocean. In the Figure 5 are presented the winds and the net heat flux forcing. The wind field shows that the stronger wind velocities are located offshore. Also strong winds are located near the coast between the 25^{o}S to 30^{o}S. The model is integrated from a state of rest (no motion) for a period of 10 days.

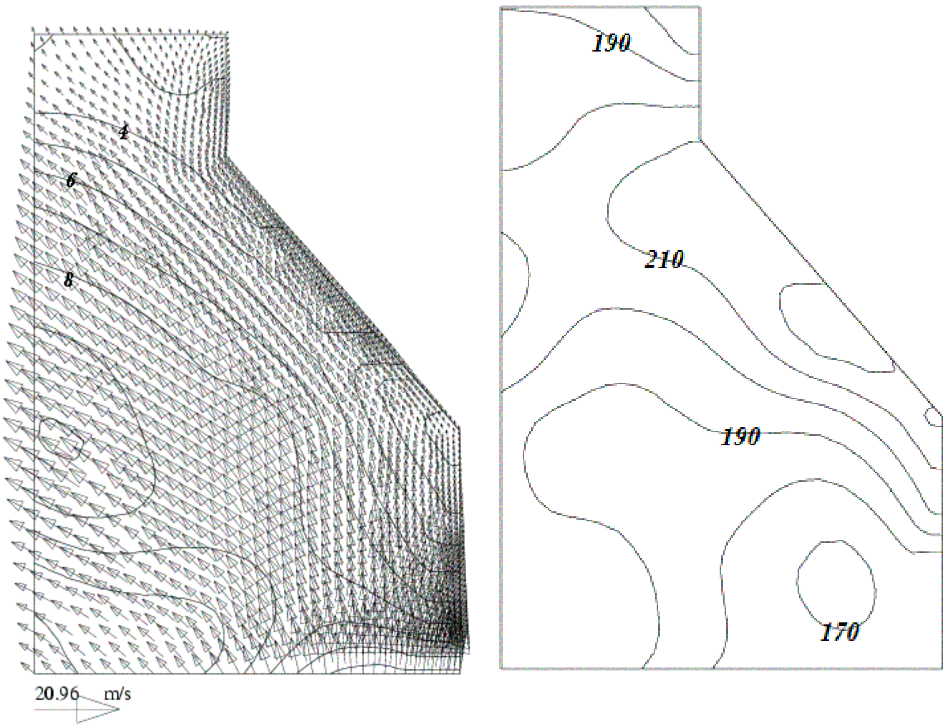

Figure 5. The Wind field and net heat flux forcings (extracted from Da Silva (1994). Left panel : The wind field forcing. Right Panel: The net heat flux $\boldsymbol{Q_n}$ (Wm^{-2}) forcing .Contours of heat each 20 Wm^{-2}. The contours of wind magnitude is 1ms^{-1} .

The Figure 6 shows the currents and SST fields calculated by the model for the month of February. The resulting pattern of the temperature contours is very similar to the observed one (compare to Figure 1, left panel). The numerical solution shows colder waters along the coastline between the 6^{o}S to 19^{o}S and from the 25^{o}S to the south. The coastal upwelling is the responsible for the lower SST along the coastal boundary. But the colder waters in the southern offshore side is not of coastal upwelling origin. It could be a consequence of the heat exchange fluxes between the atmosphere and the ocean.

The calculated SST contour of 23^{o}C describes clearly the warm water intrusion observed in the data. The temperature contours show that the warm water intrusion reaches practically the coast around the 20^{o}S, resulting a reduction of the colder pattern in this sector (between the 19^{o}S to 25^{o}S), a fact that is according to the anomalies reported by Mendelshon and Schwing (2002). The dynamical reason for the existence of warmer temperatures in this sector could be the moderate winds stress in that region and the coastline configuration change that help to the increase of the convergence pattern for northward water flow forced by strong N-S wind velocities observed around the 25^{o}S to 30^{o}S near to the coast (see Figure 5, left panel).

The current velocity field pattern shows stronger currents in a band alongshore, describing a coastal jet (Figure 6, left panel) and in the northern side. A weak component to the south is observed in the current field indicating that a superficial countercurrent is formed. In the real world, these currents are intense. The unrealistic cooling (due hydrodynamic divergence) in the northern side (0^{o}S to 6^{o}S) is not observed in the original data. This is consequence of the coastline simplification. Because in the part in front to the Guayaquil bay (from 81^{o}W to the east) the winds are eastward, a wind feature which was not captured by the schematized model due the simple straight approach.

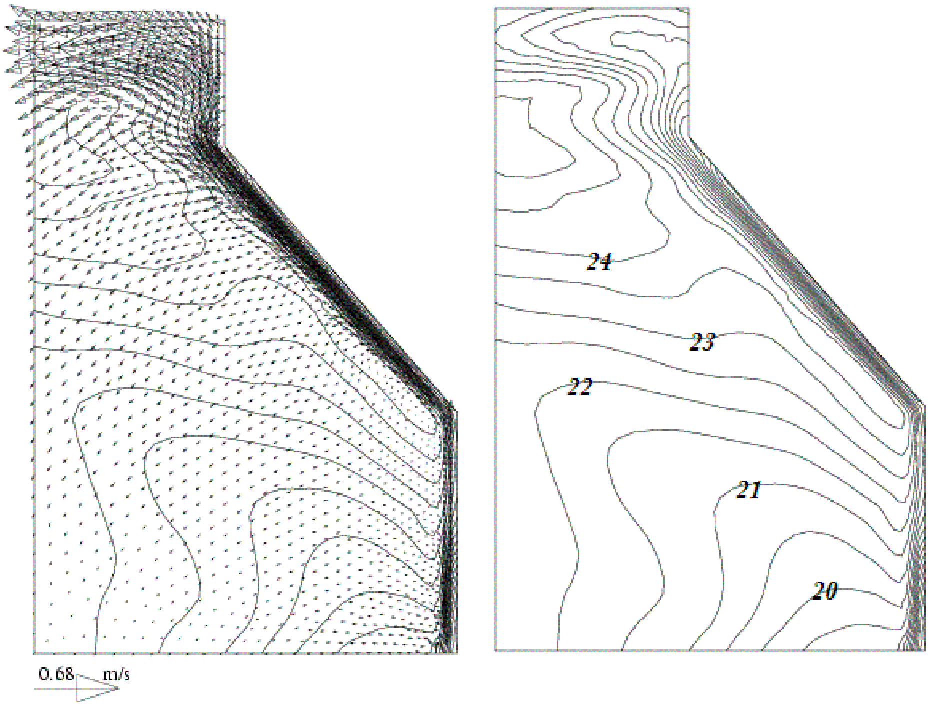

Figure 6. Solution at day 10. SST field (left panel). Velocity and SST fields (right panel).

A next step in the study of eastern pacific ocean will be the inclusion of a dynamic lower layer (2 ½ layer model) and countercurrents forcings to simulate other typical dynamic features of the eastern oceans, which are related to the sub-superficial dynamic and their interaction with the surface layer.

4. Summary and conclusions

The surface layer of stratified waters in the eastern tropical subtropical pacific ocean is modeled. The wind-driven hydro-thermodynamics model includes the momentum, continuity and heat conservation. The model consider the essential processes of a gravity reduced dynamics, with an active upper layer and a inert lower layer. The model is forced by the wind field and the heat fluxes.

The governing equations are solved applying a variational Petrov-Galerkin formulation, which includes a stabilizing operator in space and time that improves the classical Galerkin approach. The matrix $\overline{\Psi}_e$ of the stabilizing term is evaluated. The domain and variables in space and time are described by linear and continuous polynomials. At the open boundaries (sea-side) weakly reflective boundary conditions are used.

The eastern pacific ocean domain considered, extend from the equator to 30^{o}S. The schematized study area, present only the more prominent geographical coastline changes at 6^{o}S and 18^{o}S. The forcing functions, the wind field and heat fluxes were extracted from reported monthly mean data.

The model results show a concordance with the typical observed mean SST for a generic February month. Colder waters along the coastline between the 5^{o}S to 19^{o}S and from the 25^o S to the south are generated. In the sector between the 19^{o}S to 25^{o}S, the SST is warmer compared to the previous indicated sectors. The intrusion of warm water pattern from the north is simulated numerically.

The results confirm that the presented finite element model, based on a Petrov-Galerkin formulation, account for the SST description in the eastern pacific ocean.

The present paper is a first step focussing the modelling of mesoscale circulation based on the Petrov-Galerkin formulation for a finite element discretization of the ocean. The vertical structure is very simple and improvements are necessary. Particularly to simulate the complex circulation in the pacific ocean where the superficial and sub-superficial countercurrents are the main modelling challenger.

5. Acknowledgement

The present research was supported by normal funds of the LNCC during the years 2003, 2004.

6. References

Almeida R. C., Galeão A. C., Silva R.S., 1986. "Adaptive Methods for the compressible Euler and Navier-Stokes Equations", Finite Elements in Fluids , 2, 337-346, Barcelona.

Bova, S.,W., Carey G.,F., 1995. "An Entropy Variable Formulation and Petrov-Galerkin Methods for the Shallow Water Equations". In G. Carey, John Wiley, LondonEngland, Finite Element Modeling of Environmental Problems-Surface and Subsurface Flow and Transport, 85-114.

Brooks A.N., Hughes T. J. 1982. "Streamline Upwind Petrov-Galerkin Formulations for Convection-Dominated Flows with Particular Emphasis on the Incompressible Navier-Stokes Equations", Comput. Meths. Appl. Mech. Engrg. 32, 199-259.

Carbonel, C., Galeão, A. C. N. R., 2004. A Space-Time Petrov-Galerkin Model of the Upper Coastal Ocean Hydrodynamics in Limited Area Domain. Relatorio de Pesquisa e Desenvolvimento do LNCC, 10/2004.; ISSN 0101.6113.

Carbonel C. 2003. Modelling of Upwelling-Downwelling cycles caused by variable wind in a very sensitive coastal system. Continental Shelf Research, 23(16), 1559-1578.

Carbonel C., Galeão A.C., Loula A., 2000. ",Characteristic Response of Petrov-Galerkin Formulations for the Shallow Water Wave Equations". Journal of the Brazilian Society of Mechanical Sciences, Vol. XXII,No 2, 231-247.

Da Silva , A. M. M., Young C.C., Levitus S., 1994. NOAA Atlas NESDIS 6. U.S. Department of Commerce , NOAA, NESDIS.

Fofonoff N. P., 1962. Dynamics of ocean currents. In: The Sea, Ed. M.N. Hill, New York, Vol 1, 323p.

Hantel M., 1971. Zum Einfluss des Entrainmentprozesses auf the Dynamik der Oberflachenschicht in einem tropisch-subtropischen Ozean. Deutsche Hydrographische Zeitschrift. Jahrgang 24, 1971, Heft 3.

Iskandarani, M., Haidvogel, D.B., Boyd, J.P., 1995. A staggered spectral model with application to the oceanic shallow water equations. Int. J. Numer. Meth. Fluids 20, 393–414.

Mendelssohn, R., Schwing F.B., 2002. Common and uncommon trends in SST and wind stress in the California and Peru-Chile current systems. Progress in Oceanography , 53, 141–162.

Lluch-Belda, D., Schwartzlose, R. A., Serra, R., Parrish, R., Kawasaki, T., Hedgecock, D., & Crawford, R. J. M.,1992. Sardine and anchovy regime fluctuations of abundance in four regions of the world oceans: a workshop report. Fisheries Oceanography, 1, 339–347.

O'Brien J., Heburn G.W., Peffley M., Preller R., Thompson J.D., 1979. Peru Upwelling Models. Depts. of meteorology and oceanography, Florida State University, Tallahasse.

Parrish, R. H., Bakun, A., Husby, D. M., & Nelson, C. S., 1983. Comparative climatology of selected environmental processes in relation to eastern boundary current fish production. FAO Fisheries Report, 291, 731–778.

Preller, R., O'Brien, J.J., 1980. The influence of bottom topography on upwelling o€ Peru. Journal of Physical Oceanography 10, 1377-1398.

Rosenfeld L.K., Schwing F.B., Garfield N., Tracy D.E., 1994. Bifurcated flow from na upwelling center: a cold water source for Monterey Bay. Continental Shelf Research, 14(9), 931-964.

Shakib F. , 1988. "Finite Element Analysis of the Compressible Euler and Navier Stokes Equations". Phd. Thesis, Stanford University.

Yoshida Kozo, 1967. Circulation in the eastern tropical ocean with special references to upwelling and undercurrents. Japan Journal of Geophysics, 4(2), 1-75.